Event Investigation of 69 kV Double-Circuit Faults

Ahsan Mirza, Christopher Bolton, Girolamo Rosselli, and Sergio Flores
San Diego Gas & Electric®

Amanvir Sudan
Schweitzer Engineering Laboratories, Inc.

Presented at the
23rd Annual Georgia Tech Fault and Disturbance Analysis Conference
Virtual Format
April 26–27, 2021

Previously presented at the
74th Annual Conference for Protective Relay Engineers, March 2021
47th Annual Western Protective Relay Conference, October 2020

Original edition released September 2020

Event Investigation of 69 kV Double-Circuit Faults

Ahsan Mirza, Christopher Bolton, Girolamo Rosselli, and Sergio Flores, *San Diego Gas & Electric®*
Amanvir Sudan, *Schweitzer Engineering Laboratories, Inc.*

***Abstract*—Two rare yet similar faults occurred within hours on SDG&E's 69 kV parallel circuits. Because the faults involved two parallel lines, they caused unconventional fault waveforms seen by multiple relays. This, in turn, challenged the directional elements and overcurrent coordination, producing unexpected relay operations.**

This paper presents the performed investigation that helped correlate the captured fault oscillography with the type of fault. The paper explains the relay operation, focusing on the directional element, and concludes with lessons learned and suggestions for relay security improvements. The paper also emphasizes system-wide, time-coordinated event report analysis, which was indispensable to the root cause analysis.

I. Introduction

In September 2018, two faults occurred within hours of each other, and multiple breakers tripped on SDG&E's 69 kV system (Fig. 1). Because the system's close proximity to the coast exposes conductors and insulators to the salty atmosphere, some of the insulators on the system lines are rated for 88 kV. As a result, faults are rare on these lines (L12, L34, and L567).

However, on the day of the faults, heavier-than-usual fog was reported. The first fault (F1) occurred at 3:52:02 a.m., and breakers at Terminals T1, T2, T3, T4, T6, and T7 opened. Reclosing was not enabled. The patrol crew reported the fault to be within the 0.6-mile section of double-circuit Lines L12 and L34, which shared the same poles. The fault location was 1.52 miles from Terminal T1 and 0.83 miles from T4. The lines were put back into service manually.

About three hours later, at 6:55:15 a.m., a second fault (F2) occurred, resulting in the same terminals opening. This time, the patrol crew reported the fault location to be 0.18 miles farther from the location of F1 and farther from Terminals T1 and T7, but still within the same double-circuit section of the poles shared by Lines L12 and L34. Affected insulators were washed, and the lines were put back into service. Note that patrol records did not list the specific phase insulators on which the track marks were observed on the two shared lines. No such faults were reported previously or have been reported in the roughly year-and-a-half since.

This paper details the root cause investigation of these faults, explains the relay operation, and concludes with lessons learned and suggestions for relay security improvements.

II. System Overview

A. Line Lengths

All of the system lines shown in Fig. 1 are overhead conductors. Line L12 is 8.52 miles long and connects Terminals T1 and T2. Similarly, Line L34 connects Terminals T3 and T4 and is 4.6 miles long. Terminals T2 and T3 do not terminate in the same substation, but are instead connected through the rest of SDG&E's 69 kV grid comprising multiple other lines. Line L567 makes up the three-terminal line interconnecting Terminals T5, T6, and T7. The length of Line L567 from T5 to T7 is 1.89 miles. Terminal T6 is tapped at 0.5 miles from T5. In addition, Terminal T6 is itself 0.9 miles long measuring from the tapped point.

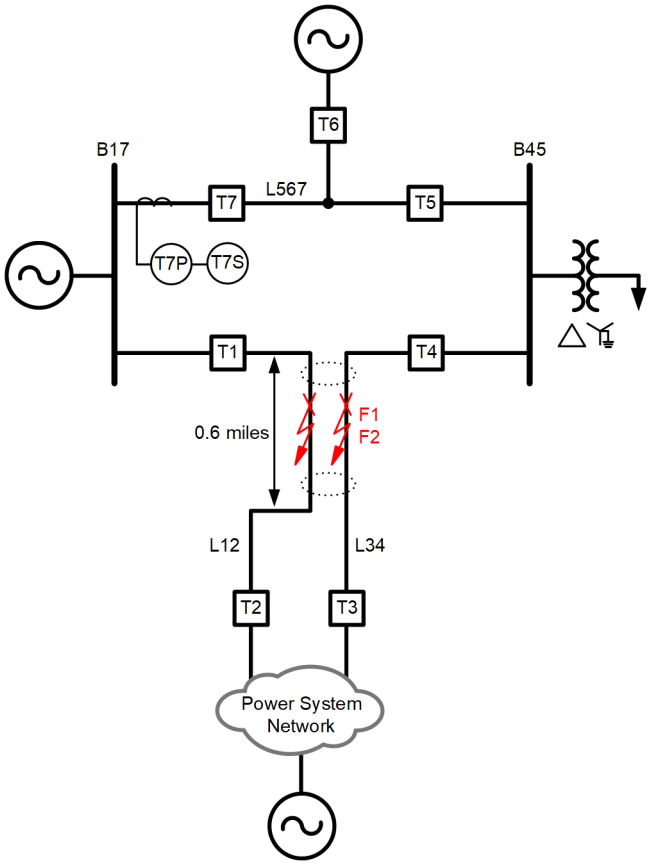

Fig. 1. SDG&E 69 kV System

B. Protection Scheme

Each terminal is protected by two relays: a primary relay and a secondary relay to provide redundant local protection. There is no delay set between the primary and secondary relay operation. A primary relay on any terminal includes 87L protection, mho phase and ground protection, and directional ground and phase overcurrent protection. A secondary relay on any terminal is identical to the primary relay on the same terminal, but does not include 87L protection. The mho element zones and overcurrent element levels are set traditionally. Zone 1 covers 80 to 85 percent of the protected line length with no time delay (similar for Level 1 of overcurrent elements). Zone 2 covers 100 percent of the line length, plus some extra

margin, with a time delay of 30 cycles to coordinate with Zone 1 of the next line. Both Zone 1 and Zone 2 are forward-looking zones.

Zone 3 is a forward-looking zone that provides backup protection to 100 percent of the length of line adjacent to the locally protected line. The Zone 3 time delay was set at 1 second. The Zone 4 phase element was also used, but only for fault direction detection purposes. It was never used for tripping.

In addition to using 87L as the primary protection for clearing faults without any intentional time delay, SDG&E also uses permissive underreaching transfer trip (PUTT) on these 69 kV lines as another way of achieving pilot protection. PUTT requires both a permissive Zone 1 element assertion to be received from the remote end relay and a local Zone 2 element assertion before a trip is declared. PUTT is typically challenging to implement on short lines because of its use of Zone 1 instantaneous elements. Since PUTT employs a smaller area mho circle in the form of its Zone 1 element, it offers less fault resistance coverage.

The ultimate protection goal for backup protection is that no fault in the 69 kV system be left uncleared for more than 1 second.

III. The Unknowns

For the two faults on the 69 kV system, we know that Lines L12 and L34 are the faulted lines. It is clear that Terminals T6 and T7 undesirably operated. T1, T2, T3, and T4, on the other hand, correctly operated and isolated the faulted line. Following are the knowns and unknowns based on the preliminary investigation:

- A-phase and B-phase on L34 and C-phase on L12 were involved in the fault. *But what type of fault was it? A case of simultaneous faults, or an intercircuit fault? Was ground involved? And what should be expected when such rare faults occur?*
- The T7 and T6 relays had undesired operations, with T7 operation triggering T6 operation. This is explained further in Section VIII. *But why did the T7 relays operate? Could we have done anything to prevent it? Were there any lessons learned?*

What follows is a paper written in a fashion that preserves the mysteries of the investigation (including the unknown fault type and root cause of the relay undesired operation). It chronologically details how the mysteries were solved. For brevity's sake, the rest of the paper is mostly centered around Fault F1, as Fault F2 was similar.

IV. T7 Primary Relay Event Report Analysis

Both relays at the T7 terminal operated unexpectedly in the same fashion. Because both the T7 primary (T7P) and T7 secondary (T7S) relays had the same settings (except that T7P had additional 87L protection functionality), shared the same current transformers (CTs) and voltage transformers (VTs), and had the same element responsible for tripping, we focus only on T7P.

Before we look at the T7P event report, the following are a couple of observations worth mentioning:

- A fault on Line L12 appears as a reverse fault for T7P, as the fault is on the line behind the relay.
- A fault on Line L34 appears as a forward fault for T7P, but far from the reach settings of mho Zone 1 and instantaneous overcurrent elements.

Based on this information, only the protection scheme of Lines L12 and L34 should have operated, not the T7 or T6 relays.

With that in mind, we delve into the event report, looking for answers to the previously posed questions.

A. Oscillography

The following analysis of captured oscillography is done as if no prior information was available from patrol crew, which is quite often the case as 1) not all physical evidence of faults are as revealing as others, making it difficult for patrol crew to find the fault, and 2) patrol crew may rely on a protection engineer to tell them first where to look for the fault based on the relay's reported fault location and event report analysis. Fig. 2 shows the current and voltage oscillography the T7P relay captured.

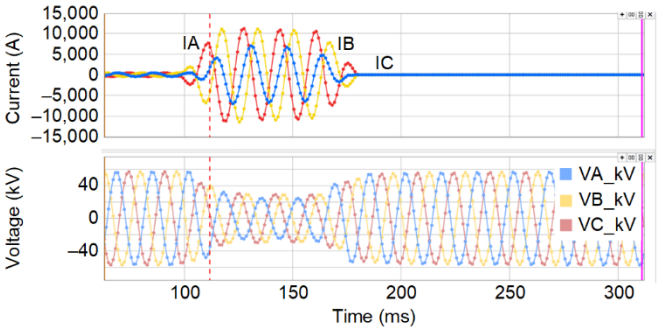

Fig. 2. T7P Relay Current and Voltage Oscillography

It is immediately clear that this oscillography reflects fault conditions, as all three phase voltages are depressed and currents are as high as 10 kA peak value. Something that also catches the eye is the unbalance in currents, even though there is high current in all three phases (reflecting that all three phases are faulted). There is slight unbalance in the voltages as well. All three phases are involved in the fault, but a conventional fault involving all three phases is a three-phase fault, which is mostly balanced in nature (ignoring the effects of line untransposition). That is not the case here, so a natural question arises: What kind of three-phase fault would create such significant current unbalance? There is little doubt that we are dealing with an unorthodox fault type.

It is interesting to see that at the intersection of the IA and IB waveforms lies the peak of the IC waveform. This waveform oddity manifests itself in the form of a clue from the current phasor diagram of Fig. 3. In the top pane, we see that the IC phasor is acting as an angular bisector of the IA and IB phasors. An additional hint as to the fault type and location is disguised in the ambiguity presented by unequal current magnitudes, where IA and IB are equal yet larger than IC. We compare this

odd current phasor relationship with that of the three-phase fault to extract meaningful information on what type of fault this could be.

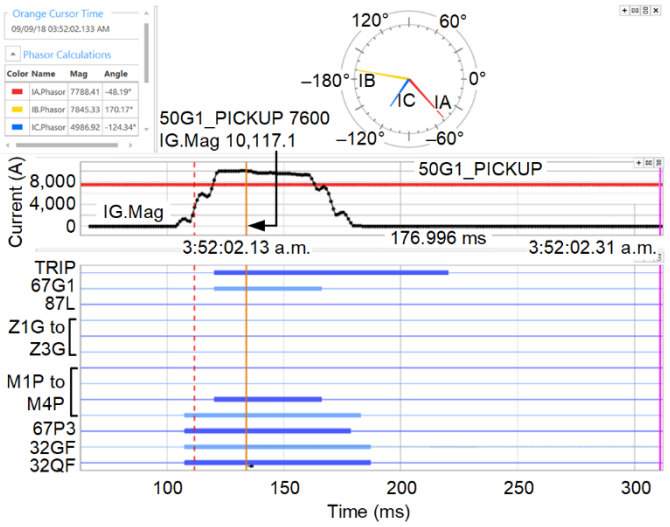

Fig. 3. T7P Relay Phasors and Protection Element Response

For a classic three-phase fault, the current magnitudes of all three phases are equal. The fact that we have equal A-phase and B-phase magnitudes but an unequal C-phase magnitude implies that A-phase and B-phase are faulted together at one location, while C-phase is faulted at another location.

Further, if the IC phasor was flipped 180 degrees from its position in Fig. 3 (and made equal to IA and IB), it would have represented a forward three-phase fault flow. (The same phasor diagram in Fig. 3 is also shown in Fig. 13 along with voltage phasors). But in reality, IC lies opposite of this forward three-phase fault position, or simply, the IC phasor lies in a reverse flow position compared with the IA and IB phasors.

What this suggests so far is a case of double faults: a forward fault from the relay location involving A-phase and B-phase, and a fault in another location behind the relay (reverse) involving C-phase.

We still cannot tell whether ground was involved in the fault or if it was an intercircuit fault or two simultaneous faults. We revisit the fault type mystery after further evaluating the T7P relay response to the fault.

B. T7P Protection Element Response

Fig. 3 also shows the response of various T7P relay protection elements to Fault F1. The 87L element did not operate, which is expected because the relay is protecting Line L567, which we know is unfaulted. The ground distance mho elements (Z1G, Z2G, and Z3G) also did not operate. However, M3P and M4P (the Zone 3 and Zone 4 phase mho distance elements) asserted, although they are not responsible for the trip. We revisit distance element response later in the paper to study it in more detail. For now, we are interested in the element that caused the trip.

The 67G1 bit (ground directional overcurrent element) asserted at the exact same time as the TRIP bit. The 67G1 assertion suggests ground involvement for this unusual fault. If we look at the phasor diagram in Fig. 3, the way IA, IB, and IC phasors are spatially arranged (which is additive in nature) leads to significant ground current (IG) calculated by the relay (the ground current is the phasor summation of IA+IB+IC). In fact, the ground current magnitude was 10.2 kA, which is above the 50G1 pickup of 7,600 A primary (middle plot in Fig. 3). For now, we know this is evidence that satisfies the overcurrent criteria of the 67G1 element. But, if this fault is suspected to be on the adjacent Line L12 (making it a reverse fault for the T7P relay), how can the forward directional evaluation criteria of 67G1 be satisfied? In other words, why would 32GF and 32QF (forward directional supervisory bits for ground overcurrent elements) assert for a fault behind the relay?

Relays use either negative-sequence voltage polarization or zero-sequence voltage polarization to determine whether a ground fault is in the forward or reverse direction. The relay settings engineer has the choice to give priority to either polarization method. There is a current-based polarization method as well, but that is not discussed in this paper because this relay was not set to use this method. The suitability of the method depends on the relay location in the power system topology [1]. The T7P relay uses negative-sequence voltage polarization as its primary method for directional evaluation, so this paper focuses solely on that method.

If a ground fault is forward, the relay's calculated negative-sequence impedance plots roughly at minus the negative-sequence impedance (–Z2S) of the source behind the relay, regardless of the distance of the fault from the relay [2]. On the other hand, if a fault is reverse, the calculated impedance plots at the positive sum of negative-sequence impedances of the protected line plus the remote source (Z2L+Z2R).

Fig. 4 illustrates this concept. The calculated point of Z2L+Z2R is fixed regardless of the distance between the reverse fault and the relay. Given the separation between the –Z2S and Z2L+Z2R points in Fig. 4, the relay uses two blinders placed between these points to distinguish whether a fault is forward or reverse. The blinder at the bottom is the forward negative-sequence threshold (Z2F). Similarly, we have threshold Z2R as the top blinder for the reverse fault detection. If the calculated negative-sequence impedance seen by the relay for a fault falls under the Z2F forward blinder threshold, the fault is forward. If the calculated impedance is above the Z2R reverse blinder threshold, the fault is reverse.

Both the Z2F and Z2R blinders are user-defined settings, best determined through system studies, although users can use automatic settings for Z2F and Z2R. The automatic settings either put Z2F and Z2R at half of the line-impedance setting, separated by 0.1 ohms [3], or at –0.3 and 0.3, respectively [4]. The T7P relay used the automatic settings, where Z2F was set at half of the line impedance and Z2R was set 0.1 ohms higher than Z2F.

Returning to the T7P event report, it is interesting to see what value of negative-sequence impedance the relay saw. The event report, however, does not provide the calculated negative-sequence impedance value by default. Instead, custom calculations are performed in the event viewer software to obtain the negative-sequence impedance value from the negative-sequence voltage (V2) and current (I2) phasors. These

two phasors are shown in the top pane of Fig. 5. Remarkably, they resemble the phasor relationship expected of a forward single-line-to-ground fault. It should be noted that the V2 and I2 phasors are obtained by the event viewer software from the captured phase voltages and currents in the event report. Since the T7P relay used A-phase as its base phase for sequence component calculation, the event viewer software was also set to use A-phase as the base phase for the plots in Fig. 5.

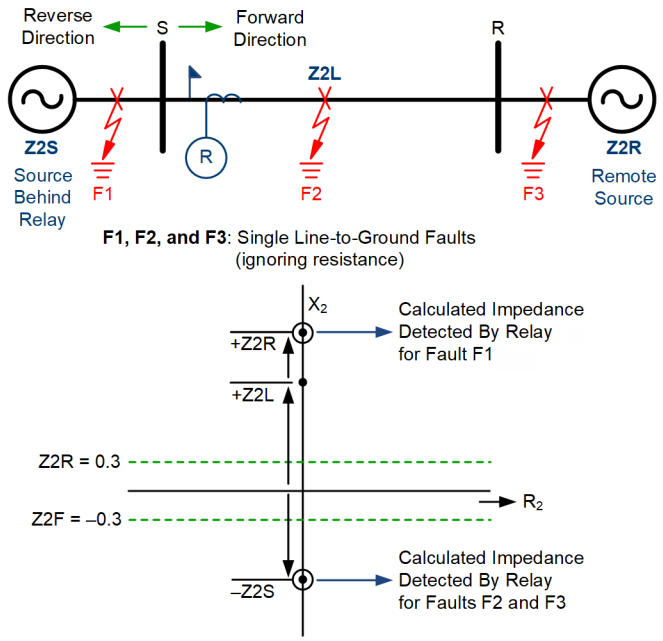

Fig. 4. Negative-Sequence Impedance Plot for a Forward and Reverse Single-Line-to-Ground Fault

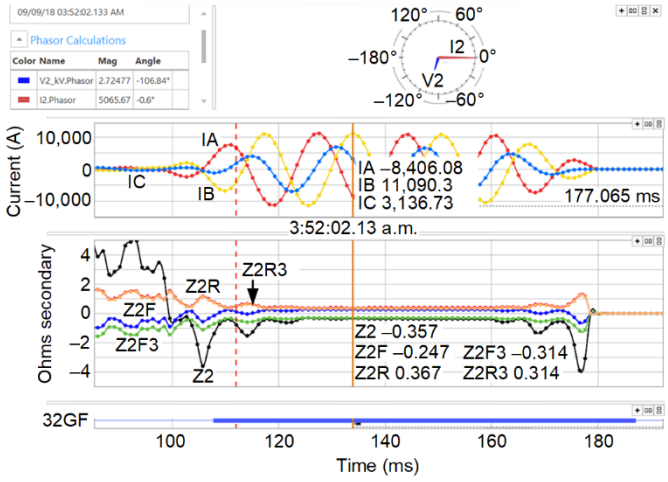

Fig. 5. Negative-Sequence Impedance Plot of T7P Relay

The plot of calculated negative-sequence impedance Z2 and the T7P relay Z2F and Z2R threshold settings are shown in Fig. 5. Clearly, the calculated Z2 (black) was well below the Z2F (blue) threshold. And even if Z2F and Z2R were moved –0.3 and 0.3 ohms, respectively (shown by Z2F3 and Z2R3 analog quantities), the calculated Z2 still lies beneath the Z2F3 (green) trace, but barely. Note that the relay adds dynamic boosts to these fixed thresholds of Z2F and Z2R, which is why traces of Z2F3 and Z2R3 are not seen at values of –0.3 and 0.3. With Z2 calculated at –0.357, Z2F at 0.247, and Z2F3 at –0.314, it is clear the Z2F3 did far better than the Z2F threshold and missed, by a fine margin, safely not declaring this fault as forward.

This negative-sequence voltage-based method of having directionality evaluation through use of Z2F and Z2R blinders banks on the fact that impedances will lie either close to –Z2S or Z2L+Z2R depending on fault direction. It is worth mentioning that this method is based on sequence component derivation for a conventional single-line-to-ground fault. If a fault is not a conventional fault (which is the case for the fault we are analyzing), then this directional element method may not work. At the same time, unconventional faults such as this are quite uncommon.

At this point, it could be deduced that the relay operated because it saw ground current magnitude larger than the threshold it was set at, and the calculated negative-sequence impedance dropped below the set threshold, indicating a forward fault. However, that does not answer why the relay would see such large ground current and why the negative-sequence impedance would drop low (or how V2 and I2 still line up like a conventional forward single-line-to-ground fault even though we know this fault involves phases on two double-circuit lines).

To answer these questions, we first must find what kind of unconventional fault this is. The investigation changes course here to focus on finding the fault type.

V. Fault Type

We start by laying out the one-line diagram of the system in Fig. 1 and opening event reports for secondary relays, this time at Terminals T1, T2, T3, and T4. Recall that the primary and secondary relays at each of the four terminals share the same CTs and VTs.

Fig. 6 shows the oscillography and phasors from two combined event reports of the T1 secondary (T1S) and T2 secondary (T2S) relays. The C-phase currents are high at around 11.7 kA and 3.29 kA for the T1S and T2S relays, respectively. Moreover, both IC phasors lag their respective VC phasors by roughly 75 degrees. This pointed toward an internal fault on Line L12 involving at least C-phase. On the other hand, A-phase and B-phase seem unfaulted. This is evident from their relatively low magnitudes compared to C-phase and the fact that IA at T1 (1,049.21 ∠–58.53 A) is roughly equal in magnitude to IA at T2 (1,045.67 ∠123.11 A), but near 180 degrees out of phase in angle. The same observation could be made for the B-phase current phasor.

Combining two event reports in the event viewer software is only valid if the individual event reports were already time-synchronized with a high-accuracy time source (e.g., IRIG-B signal from Global Positioning System [GPS] clock), which in turn happens only if the relays were time-synchronized at the time of the event. Both of these event reports had their Time-Synchronized OK (TSOK) bits asserted, confirming relays were synchronized with a high-accuracy time signal at the time of Fault F1.

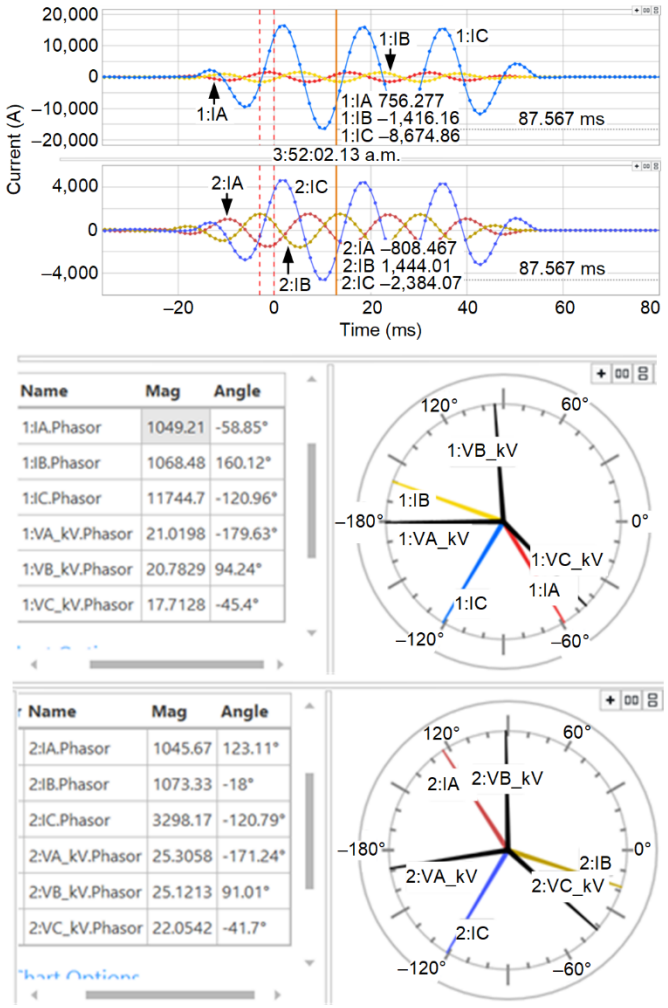

Fig. 6. T1S and T2S Combined Event Reports

Next, we examine the fault oscillography captured by the T3 secondary (T3S) and T4 secondary (T4S) relays protecting Line L34. These are shown in Fig. 7 and Fig. 8, respectively. The T3S and T4S relay event reports could not be combined because the T4S relay was not time-synchronized when the fault occurred. This was evident from deassertion of TSOK in the T4S event report. However, this does not prevent us from concluding that A-phase and B-phase are faulted and C-phase is not. This can be deduced by comparing C-phase current phasor magnitudes in Fig. 7 (IC is at 2,144.3) and Fig. 8 (IC is at 2,143.86 A). Additionally, IC is lagging VC by 78.6 degrees at Terminal T3, whereas IC is leading VC by 105.25 degrees at T4. This implies current IC flows in through T3, lagging VC by 78.6 degrees, and flows out of T4, lagging VC by 74.75 degrees (180–105.25= 74.75 degrees). On the contrary, A-phase and B-phase current magnitudes are different on either terminal and significantly larger than IC. IA is 9.5 kA at T3 and IA is 11.3 kA at T4, with similar magnitudes for IB. The IA and IB angular relationship with its corresponding phase voltages (VA and VB) is not immediately clear to explain the type of fault on Line L34. However, the closest resemblance of a fault type would be an A-phase-to-B-phase-to-ground (ABG) fault, but we cannot say with certainty if that is indeed the fault type.

To summarize what we have found so far, Line L12 has a C-phase internal fault, and its A-phase and B-phase currents seem to be carrying fault current (for a fault somewhere else), but the current is flowing in and out of the line. Line L34, on the other hand, has an internal fault involving A-phase and B-phase, and C-phase seems to again be carrying fault current (for a fault somewhere else) because the current is flowing in and out of the line.

A clear pattern has emerged. Lines L12 and L34, besides feeding current into their internal faults (C-phase, and A-phase and B-phase, respectively), are also carrying fault current contribution for the other line. For example, L12, besides feeding its internal C-phase fault, is also carrying current on its A-phase and B-phase to feed into the L34 internal fault involving A-phase and B-phase.

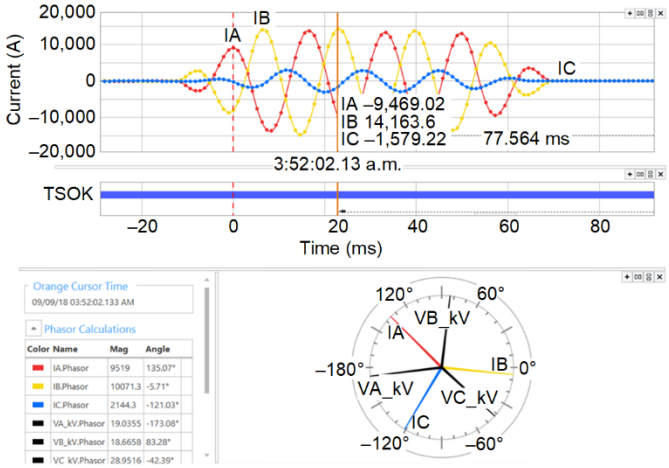

Fig. 7. T3S Event Report

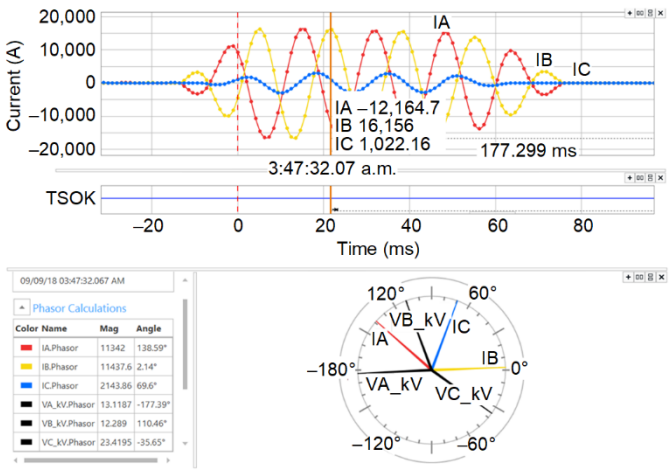

Fig. 8. T4S Event Report

To determine the fault type, we start by exploring two possibilities:

- There was an intercircuit fault between C-phase of L12 and A-phase and B-phase of L34 that did not involve ground.
- There were simultaneous faults, with a C-phase-to-ground (CG) fault on Line L12 and an ABG fault on Line L34.

If neither option makes sense, we search on. There is no difference between the two options except that one involves ground and the other does not. A simultaneous fault is a case of an intercircuit fault bridged through ground, with some current escaping back through ground.

A. An Intercircuit Fault (Phase Only, No Ground)

We start by exploring the option of an intercircuit fault between Lines L12 and L34 shared on the same poles. A flashover between multiple phases of two lines in close proximity to each other (due to shared poles) seems plausible.

To start, we transform the one-line diagram of Fig. 1 into its three-phase view and place a short between C-phase of L12 and A-phase and B-phase of L34, as shown in Fig. 9.

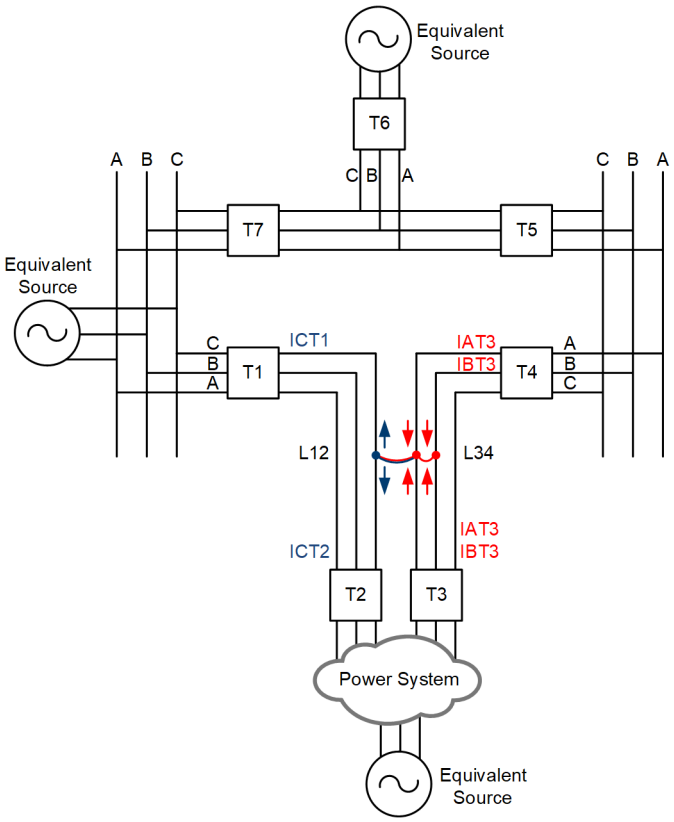

Fig. 9. Intercircuit Fault Illustration

To find out if this is an intercircuit fault, we take the Kirchhoff's Current Law (KCL) approach. If it is indeed a case of an intercircuit fault with no ground involved, then adding all the current flows into the fault point should give us a value of zero in accordance with KCL. If the currents add up to a significant non-zero value, then that non-zero value represents the ground current, and it is instead a case of a double-circuit fault involving ground.

The currents to add up are C-phase currents at T1 and T2 (shown as ICT1 and ICT2 in Fig. 9), and IA and IB pairs at T3 and T4 (shown as IAT3, IBT3, IAT4, and IBT4, respectively, in Fig. 9). To add the currents, we simply combine the event reports from the T1, T2, T3, and T4 relays and perform custom calculations in the event viewer software to obtain the KCL summation in (1).

$$ICT1 + ICT2 + IAT3 + IBT3 + IAT4 + IBT4 = 0 \quad (1)$$

For this summation to provide valid results, all event reports must be time-synchronized. Unfortunately, the T4 relays were not time-synchronized at the time of the fault. T1, T2, and T3 were time-synchronized.

However, the T4P relay is the remote 87L partner relay for T3P (to protect Line L34), so the T3P event report should have captured remote 87L currents as well. So, an attempt was made to obtain IAT4 and IBT4 currents by opening T3P's event report (shown in Fig. 10). Surprisingly, both of T3P's local (IAL, IBL, and ICL) and remote (IAY, IBY, and ICY) 87L currents abruptly disappeared after the first two cycles.

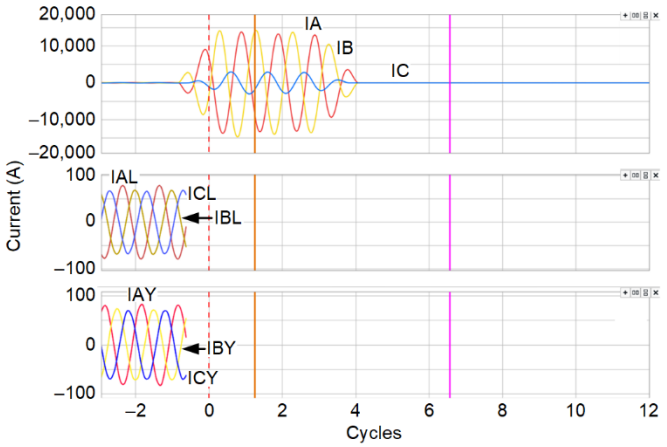

Fig. 10. T3P Event Report Showing Local and Remote 87L Currents

IAY would have given us time-shifted IAT4 and IBY time-shifted IBT4 because the T3P and T4P relays did not require the use of the GPS time signal for their 87L function. The 87L function was instead based on the ping-pong method, which relies on fixed and deterministic 87L channel latency between T3P and T4P. The 87L current values are time-shifted based on the channel latency.

But these currents came to a halt while they were in their load current states. This is unexpected, and once again halts the investigation. Why would the remote currents disappear? And why at the time when they are needed the most, during a power system fault? We revisit the 87L issue later in the paper. For now, we look for an alternative way to determine intercircuit fault possibility through use of (1).

Can we still figure out a way to verify the validity of (1)? Maybe we can if we only compare the magnitudes. If IRIG-B was present at all four terminals, we would have gotten the summation result of (1) in the form of a number—a complex number, to be precise, that has a magnitude and an angle. With the absence of IRIG-B, we cannot determine the angle of the summation result, but can at least compare the magnitudes of either side of (2) (derived from (1)).

$$ICT1 + ICT2 + IAT3 + IBT3 = -(IAT4 + IBT4) \quad (2)$$

Next, denoting the left side of (2) IfT123 and the right hand side IfT4, we get (3).

$$IfT123 = -IfT4 \quad (3)$$

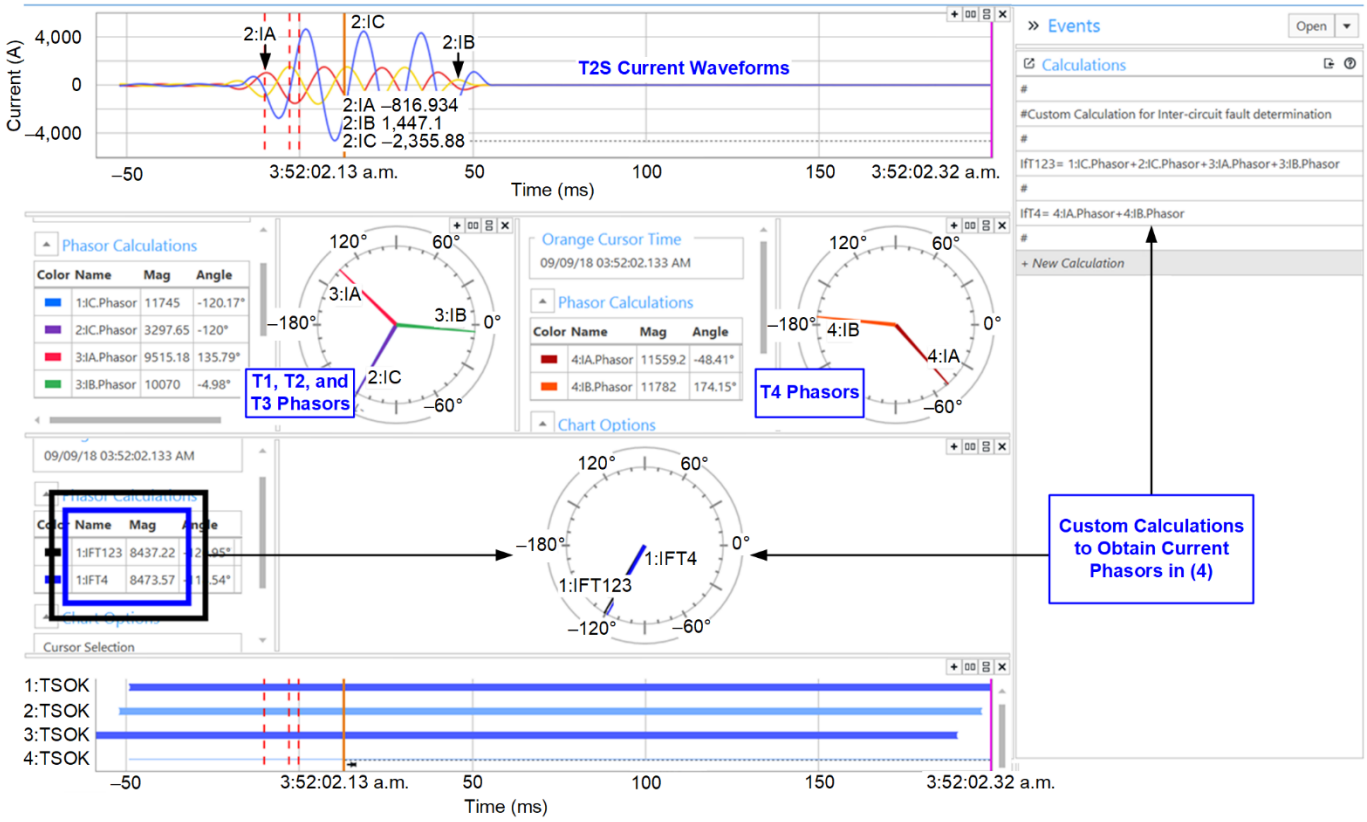

Fig. 11. Combined Event Reports to Form (4)

Finally, rewriting the equation in polar representation, we get (4).

$$|\mathrm{IfT123}|\angle\alpha = |\mathrm{IfT4}|\angle\beta + 180 \tag{4}$$

We proceed further and combine all four event reports from T1S, T2S, T3S, and T4S in the event viewer software and perform custom calculations to form (4). Fig. 11 shows the result of the two phasors (IfT123 and IfT4). The two current magnitudes are quite close to each other at 8,437 A for IfT123 and 8,473 A for IfT4. Such close magnitudes indicate that ground was possibly not involved, and the fault was instead a phase-only intercircuit fault between C-phase of L12 and A-phase and B-phase of L34.

Though the calculations and analysis suggest no involvement of ground, we wanted additional proof that did not rely on calculations, so we looked for currents that may have flowed in a neutral-to-ground connection of a wye-delta transformer. Terminal T3 substation digital fault recorder records were explored. There were a couple of 69/230 kV transformer banks (grounded wye-delta) whose captured neutral current was recorded at about 1,500 A. This is a clear indication that ground was somehow involved in the fault.

Now, the questions are: Why did the event analysis employing (4) wrongly predict no ground involvement, and was the ground involved simultaneously to make it a case of simultaneous CG and ABG faults?

To answer these questions, we pursue ways to time-align the T4 relays' event reports.

B. A Case of Simultaneous Faults Involving Ground

We start by drawing the three-phase current flow distribution that would best represent the simultaneous double-circuit faults. Fig. 12 captures this hypothetical per-phase current flow.

The presented current distribution also shows how the relays at terminals like T7 can see forward flows on A-phase and B-phase and a reverse flow on C-phase. This explains and matches T7P's current phasors shown in Fig. 3.

Since the fault on Line L34 only involves A-phase and B-phase, the C-phase is unscathed, as is evident by magnitudes of 2,144 A seen at both terminals of T3 and T4 (see Fig. 7 and Fig. 8). The magnitudes being equal suggests current came in through one terminal and out of the other, matching the current flow distribution in Fig. 12.

Now, if the T4P was time-synchronized, its corresponding event report would have shown its IC current (and phasor) to be exactly opposite, or 180 degrees out of phase with T3P's IC current phasor. We use this fact to manually time-align the T4P event report in the event viewer software so that both T3P and T4P IC current phasors are 180 degrees out of phase of each other. Fig. 13 shows 3:IC.Phasor and 4:IC.Phasor, corresponding to T3P and T4P, respectively, as almost 180 degrees out of phase with each other resultant of this time alignment.

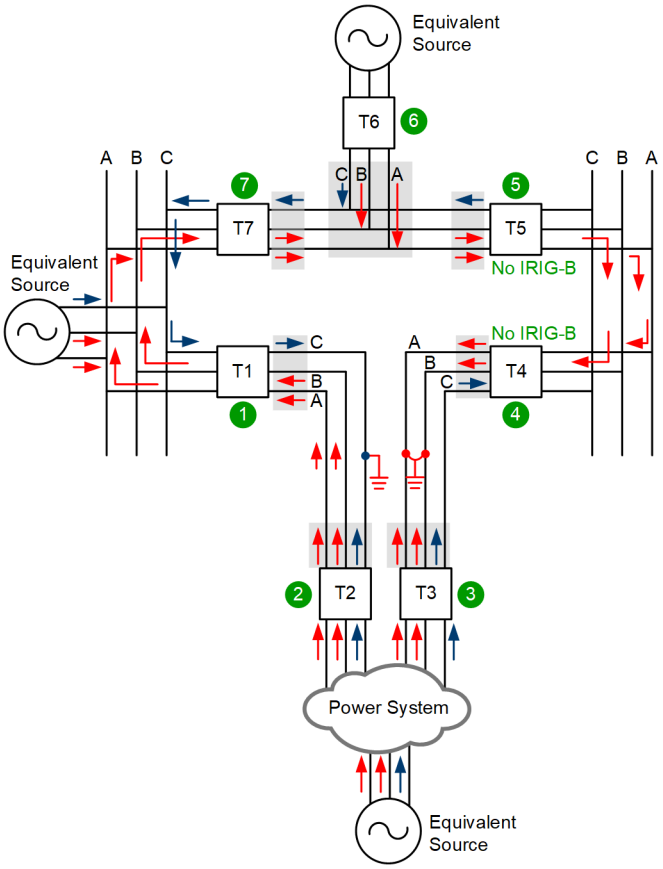

Fig. 12. Hypothetical Three-Phase Current Flow for Simultaneous Double-Circuit Ground Faults

Now that T4P has been time-aligned, the T5P relay (which also did not have time synchronization present) event report can also be time-aligned using the voltage waveforms. (Because both T4P and T5P were in the same substation connected to the same bus [B45], they shared the same set of VTs).

Fig. 13 shows all seven terminals' phasors together with all the event reports time-aligned.

A close examination of phasors in Fig. 13 reveals current flow distribution matching Fig. 12.

Returning to our investigation to determine simultaneous ground fault possibility, we formulate (1) in the form of (5).

$$IGND = ICT1 + ICT2 + IAT3 + IBT3 + IAT4 + IBT4 \quad (5)$$

Fig. 14 shows the phasor value of IGND obtained through custom calculations in the event viewer software.

Not surprisingly, we still have roughly the same magnitudes of 8,453 and 8,454 A of IfT123 and IfT4, respectively, just like we saw in Fig. 11. But now we know their respective angles (now that all the event reports have been time-aligned) as well. IfT123 and IfT4 are roughly 170 degrees apart from each other, The 10-degree difference (180–170 degrees) is enough to reveal the existence of ground current of ~1,423 A.

If it was strictly a phase-only intercircuit fault, then IfT123 and IfT4 would have been 180 degrees respective of each other, and no current would have escaped to ground.

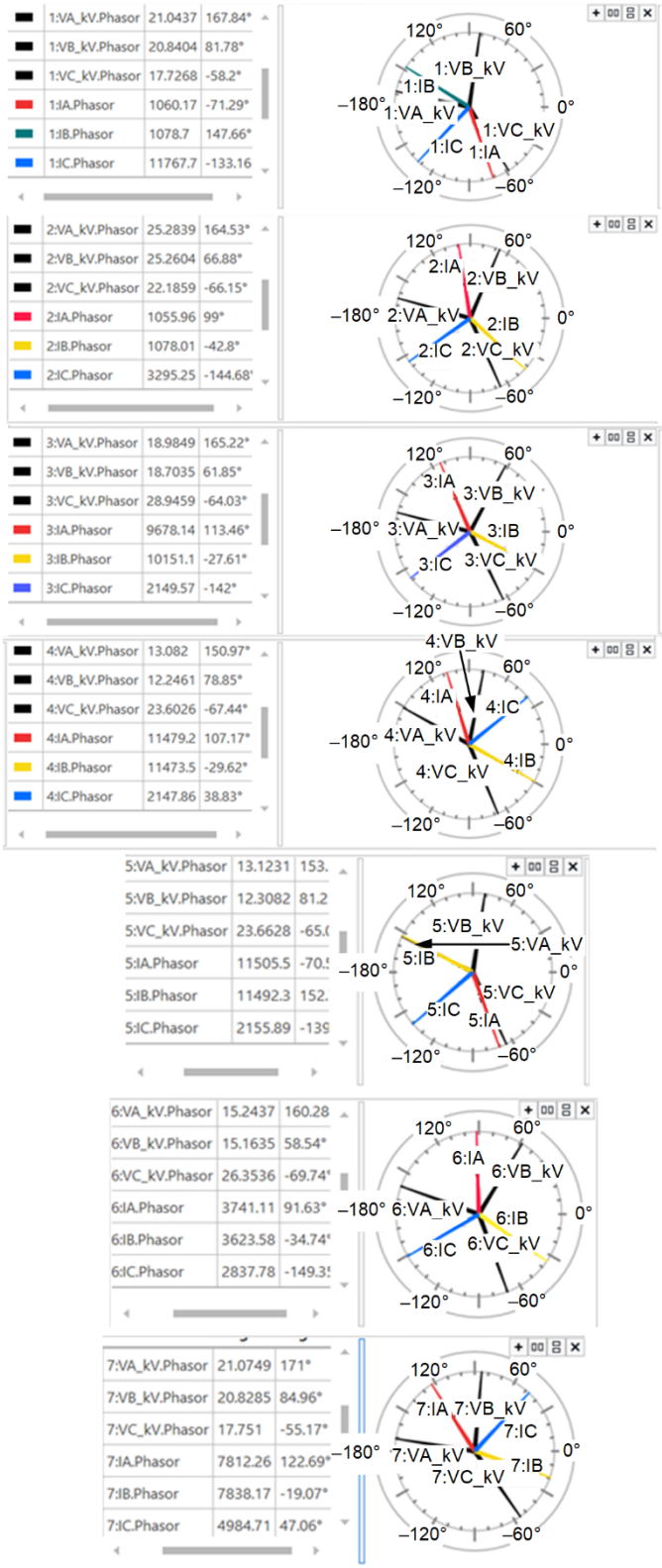

Fig. 13. Global Phasor View From Combined Time-Aligned Event Reports of All Seven Terminals

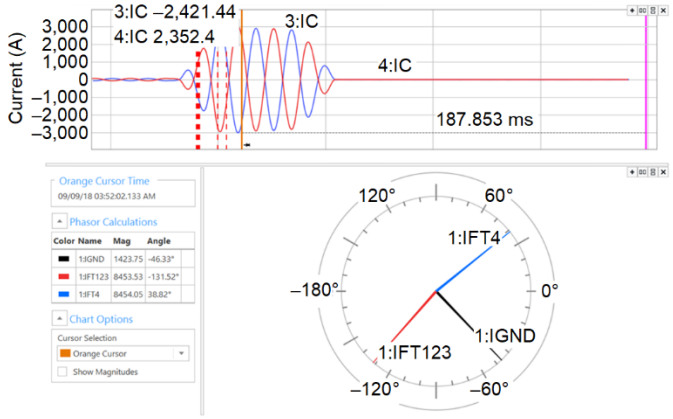

Fig. 14. Ground Current (IGND) of (5) Obtained Through Event Report Custom Calculations and Time Alignment

VI. 87L Element Behavior

As noted in the previous section, the T3 and T4 relays did not operate on their 87L elements for the internal fault on Line L34 like they should have. Upon further investigation, it was found that the Receive 87L data OK from Channel Y (ROKY) bit in the T3P relay had deasserted just a few milliseconds after fault inception (Fig. 15). Channel Y is the communications channel through which T3P exchanged 87L data with T4P on the other end of L34. ROKY deassertion is an indication of a potential communication problem with Channel Y, which causes the 87L element in the T3P relay to be disabled. One manifestation of 87L disablement appears in the form of the vanishing of IAL, IBL, and ICL (87L local phase currents of T3P) and IAY, IBY, and ICY (87L remote phase currents of T3P; that is, local current of T4P obtained via Channel Y), as shown in Fig. 15.

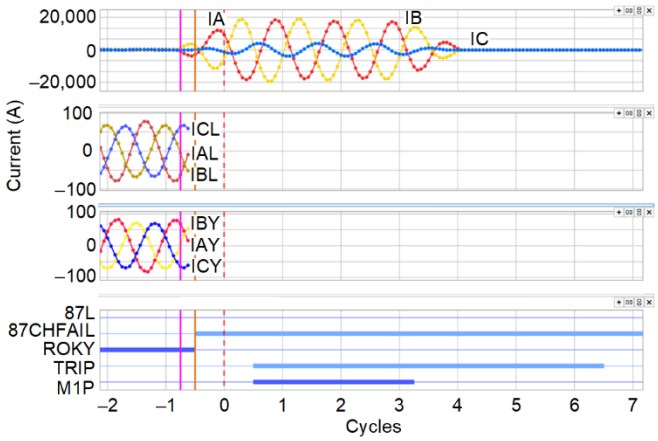

Fig. 15. T3P Event Report Showing 87L Element Behavior

While 87L disappears right when the fault starts, M1P (Zone 1 phase mho distance element) fortunately comes to the rescue and operates in about 1.25 cycles, clearing the fault. This showcases the importance of having local backup protection elements.

Next, we decide to investigate 87L element behavior in the other line relays out of curiosity. Recall that the 87L elements of the Line L567 relays remained secure for the external faults on Lines L12 and L34. When we plot ROKX and ROKY bits (Channel X and Channel Y health indicators) for the T7P relay, they surprisingly turn out to also be deasserting right when the fault starts. So, the 87L element remained secure because there was potentially an 87L channel problem at the same time of the double-circuit faults. It cannot be a mere coincidence that 87L elements were disabled simultaneously in multiple relays (T3P, T7P, and so on) due to potential channel problems, especially when it all seems to be triggered by the fault inception.

To get to the root of the issue, we decide to plot ROK bits of all seven relays together. The bottom portion of Fig. 16 shows the pertinent ROK bits of all seven 87L relays (T1P, T2P, and so on) combined.

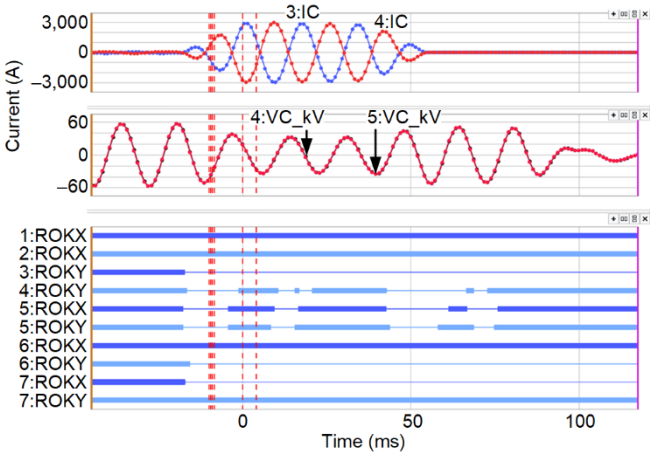

Fig. 16. Combined Event Report of All Seven 87L Relays Showing ROK Bits

Digital bits and analog quantities from different relays are identified using the colon notation. For instance, 1:ROKX represents the ROKX bit of the relay T1P. Similarly, 4:IC represents the IC current of the T4P relay.

In Fig. 16, T1P's ROKX and T2P's ROKX bits remain asserted during the fault. This indicates that the 87L communications channel used to protect Line L12 is unaffected by the double-circuit faults. Next, T6P's ROKX and T7P's ROKY bits are unaffected. Both of these bits represented the health of the same 87L communications channel, even though bits seem to indicate a Channel X and Channel Y. It is just a different naming convention followed by the T6P and T7P relays. In summary, the 87L channel between the T6P and T7P relays is unaffected by the double-circuit faults.

All of the remaining bits in Fig. 16 do not stay asserted after the fault inception. These bits represent the three 87L channels between T5P and T6P, T5P and T7P, and T4P and T3P. Furthermore, T4P's ROKY bit and T5P's ROKX and ROKY bits are intermittently asserting and deasserting.

Based on this behavior, we look for the commonality in the data and observe that channels connecting the T4P and T5P relays are the ones affected. The T4P and T5P relays belong to the same substation and therefore must be using the same communications equipment or technology—perhaps the root cause behind the 87L element disruption at multiple relays. The 87L elements of T1P and T2P were intact perhaps because they used a communications channel independent of communication equipment and media at the B45 substation.

It turns out that the affected 87L channels used leased telecommunication lines involving copper wires. Further digging revealed that the communications channels at T4 and T5 had dropped out in similar fashion for faults prior to double-circuit faults.

In previous sections, we covered the directional element response for the T7P and T7S relays, and in this section, we discussed the 87L element behavior for all relays. Next, we focus on one of the main backup protection functions—the phase and ground mho distance (21) elements—to see how they operated for the double-circuit fault(s).

VII. Mho Distance Element Behavior

Reference [5] describes how a mho distance element is implemented in modern microprocessor-based relays. There are many components that collectively form a mho distance element. Among them and relevant to double-circuit fault event analysis are the following:

- Impedance calculation and comparison to the reach (pickup) setting
- Directional element supervision
- Faulted identification selection (FIDS) algorithm

Reference [6] illustrates how the impedance calculation and comparison translate to the R-X plane in the form of a circle. The required directional element supervision has the effect of increasing the security of the mho element. Lastly, the FIDS algorithm is used to enable only two of six distance elements (AG, BG, CG, AB, BC, and CA) by comparing the zero-sequence current (I0) angle with the negative-sequence current (I2) angle. The FIDS logic has the effect to again increase the overall security of the mho distance element by disabling individual distance elements for unfaulted phases. Reference [7] provides more details on this.

With this essential information in mind, we begin to evaluate the response of the distance elements (21P and 21G) in all relays at the seven terminals to the double-circuit fault. We start by looking at what we expect the distance elements to do for these double-circuit faults.

The double-circuit faults are internal to Lines L12 and L34. C-phase is faulted in Line L12. A-phase and B-phase are the faulted phases in Line L34. Line L567 is unfaulted. Hence, we expect the following:

- At least a couple of Zone 1 mho element assertions from the four relay pairs at T1, T2, T3, and T4.
- An AB distance element pair (MAB*n*, where n=1 or 2) to assert for relay pairs at T3 and T4.
- A CG distance element (Z*n*G, where n=1 or 2) to assert for relay pairs at T1 and T2.
- No assertion of Zone 1 element in any of the relay pairs at T5, T6, and T7, as the double-circuit faults are external to Line L567.

We start with the relay pair at T7. As before, since both relays (T7P and T7S) shared the same VT and CT and had the same settings, we show the mho element(s) response for T7P only.

Fig. 17 shows the mho element response for the Zone 1, Zone 2, and Zone 3 mho phase elements of ZAB and the mho ground elements of ZCG. The reason we show ZAB and ZCG (and not ZBC, ZCA, ZAG, and ZBG) is because only ZAB and ZCG are enabled by the relay during the fault. This is evident by FSC assertion and deassertions of FSA and FSB. FS*n* (n=A, B, or C) is the output bit of the FIDS algorithm described in [7] that determines which two mho elements out of six to enable. The FSC assertion from a relay standpoint represents the fact that either there is a CG fault *or* there is an ABG fault. Interestingly, FSC has asserted when *both* fault types are present. This correct determination can be attributed to the spatial displacement of the I0 and I2 phasors. For a CG or ABG fault, I2 leads the I0 phasor by roughly 120 degrees. And in this case of a double-circuit fault, the same angular relationship between I2 and I0 is observed (Fig. 17) at T7.

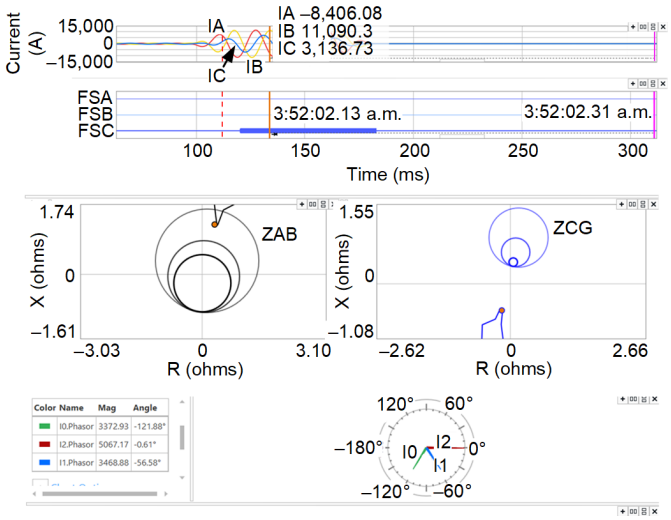

Fig. 17. T7P Mho Element Response

First, we break down the double-circuit fault(s) into two individual faults, one on Line L34 and one on Line L12. The fault on L34 involving A-phase and B-phase is forward with respect to T7P. This manifests in the R-X impedance plane (ZAB in Fig. 17) with the operating point (orange dot) lying in the first quadrant. The first quadrant of the R-X plane symbolizes forward direction of fault current flow. The operating point is well outside the Zone 1 and Zone 2 mho circles but within Zone 3.

Next, the fault involving C-phase on Line L12 is a reverse fault for relay T7P. This manifests in the R-X impedance plane (ZCG in Fig. 17) with the operating point (orange dot) lying in the third quadrant, which symbolizes a reverse fault current flow. The operating point is well outside all three mho circle zones.

This suggests that T7P has successfully captured the imprint of the fault type in the form of its ZAB and ZCG mho plots. Perhaps, more importantly, both the mho elements correctly declared the fault to be outside the protected Line L567.

Like the T7P relay, we evaluated the mho element response of the remaining relays as well. There were two noteworthy observations: FIDS operations and mho element operations.

A. FIDS Operations

Fig. 18 shows the FIDS logic response in the form of FSC bits for all seven relays (only primary relays shown). Not shown in Fig. 18 are the FSA and FSB bits, which remained deasserted. Once again, FSC assertion indicates either a CG or ABG fault from a relay standpoint. Every relay asserted its FSC bit (which was arguably a correct assertion) except the relays at Terminal T3.

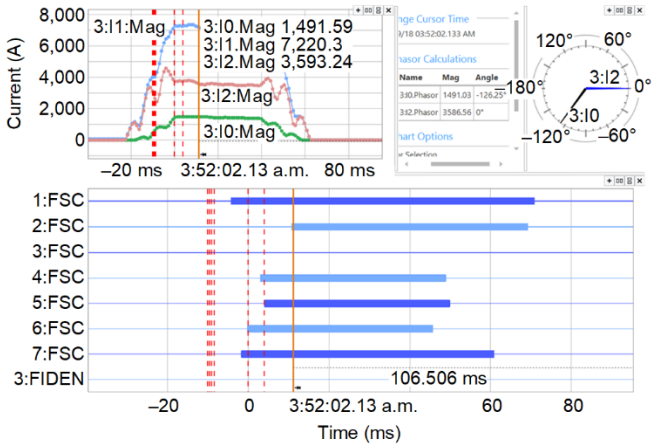

Fig. 18. Combined Event Report of All Seven Terminals Showing Respective FIDS Logic Response

Fig. 18 also shows that I2 leads I0 by roughly 120 degrees, but still FSC did not assert. Why? The fault identification logic is designed to detect faults that involve ground. The zero-sequence current and zero-sequence voltage measured by T3P for this fault were not of sufficient magnitude to enable the FIDS logic. This is evident by the FIDS enable bit, 3:FIDEN in Fig. 18, never asserting.

It is worth noting that the AB phase-to-phase mho element is not blocked by the assertion of FSC, but rather by assertions of either FSA or FSB. Thus, had FIDEN and FSC both asserted, it would not have prevented T3P's operation. The assertion of FSC blocks the AG, BG, CA, and BC mho elements.

B. Mho Element Operations

We observed that the mho elements of relays at T5 and T6 remained secured, as expected. Mho elements of relays at T1, T3, and T4 operated as expected. What was not expected was the mho element dormancy for the T2 relays. There was an internal fault on Line L12 protected by T2P and T2S, so their mho elements should have operated. Fig. 19 shows Z1G in T2P remaining deasserted throughout the event duration. Why?

We investigate the deassertion of the T2P Z1G element by exploring the three core components of a mho element previously discussed. The 2:FSC bit assertion in Fig. 18 showed the FIDS component of the Z1G mho element working correctly. Further, the top pane of Fig. 20 shows the impedance calculation of ZCG. The operating point (orange dot) lies within the Zone 1 mho circle, which proves the impedance calculation portion of the Z1G mho element is also working correctly. The last portion to evaluate is the forward directional element supervision portion. Fig. 20 shows the 32GF (forward direction) and 32GR (reverse direction) bits of the T2P relay. Unbeknownst to us, T2P's directional evaluation was challenged as well, although in a contrary fashion to T7P. T2P saw the forward (internal) fault on Line L12 as a reverse fault (evident by 32GR assertion), and therefore did not allow supervision for the Z1G mho element. The negative-sequence impedance (Z2) calculation for T2P's directional element is also shown in Fig. 20. Z2 is computed as 1.919 secondary ohms by T2P and is barely (yet clearly) above the Z2R setting value of 1.859. Why?

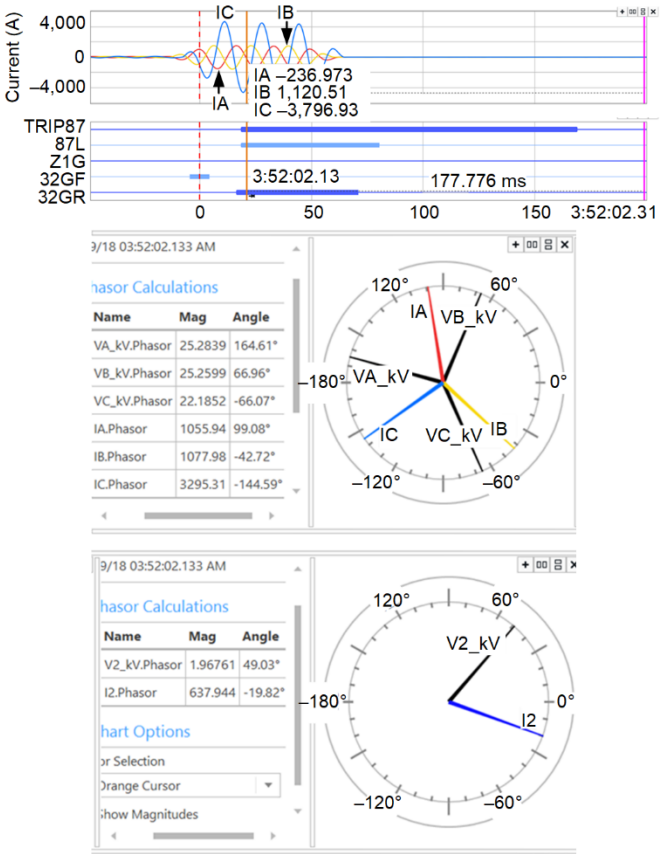

Fig. 19. T2P Event Report Showing Mho Ground Zone 1 (Z1G) Element Remaining Deasserted

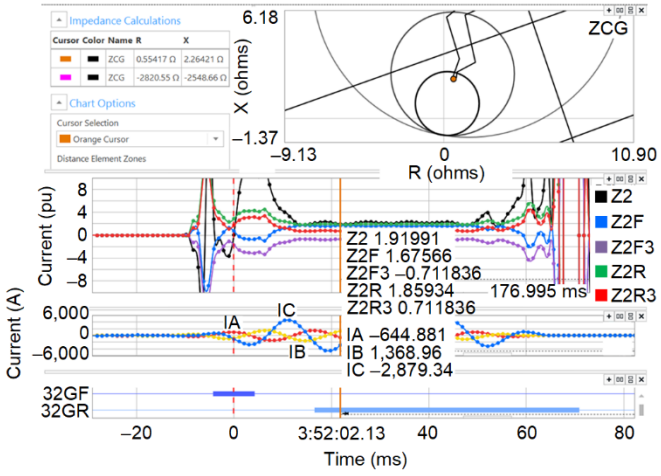

Fig. 20. Negative-Sequence Impedance Calculation of T2P Relay

The answer lies in the negative-sequence voltage (V2) and current (I2) values seen by the relay for the double-circuit fault. In Fig. 19, which shows V2 and I2 phasors as seen by T2P, V2 leads I2 with an angle less than 90 degrees. This is, in fact, the V2 and I2 relationship expected for a reverse single-line-to-ground (SLG) fault! This rare double-circuit fault has been successful yet again in challenging the relay directional element, this time by hiding the forward directionality of the fault.

VIII. T6P Operation

T6P unexpectedly operated for the external double-circuit faults as follows: the assertion of the underreaching 67G1 bit in T7P was used as one of the conditions to send a permissive transfer trip signal to T6P. And, with T6P's forward-looking overreaching elements also asserting for the double-circuit faults, the criteria was satisfied for T6P tripping under the PUTT scheme.

Note that a PUTT scheme on a three-terminal line requires a permissive transfer trip signal from any of the other two terminals (e.g., T6 could trip if it receives permission from either T7 or T5) because the permissive signal is derived from underreaching Zone 1 or instantaneous overcurrent elements. This contrasts with how directional comparison blocking (DCB) and permissive overreaching transfer trip (POTT) schemes function. Both schemes would have prevented T6 from operating. If a DCB scheme was used, T5 would have sent a blocking signal to T6 because the T5 mho impedance calculation plotted in the reverse direction. If a POTT scheme was used, T5 would never have sent a permissive signal because its forward-looking overreaching zone would never have picked up for a mho impedance that plots in reverse. Under a POTT scheme, permissive signals from both T7 and T5 would have been required.

IX. Conclusion

Following is a summary of our findings and lessons learned:

- The 67G1 element of the T7P relay protecting Line L567 operated because it was set too sensitive and because of the nature of the fault. The double-circuit fault caused forward flow on A-phase and B-phase and a reverse C-phase flow, which led to higher ground current (calculated by the relay) than there actually was. This is because of the spatial arrangement of IA and IB and the reverse flowing IC current was additive in nature, hence the larger-than-actual IG ground current (Fig. 3).
- The three-terminal Line L567 is a short line, so the instantaneous overcurrent and Zone 1 distance elements should have been set with the utmost caution, focusing on security.
- The directional element at the T7P relay saw the reverse CG fault on Line L12 as forward. This is because the V2 and I2 relationship observed by T7P is surprisingly the signature of the V2 and I2 relationship for a conventional forward SLG fault. It should not be forgotten that at the same time, there were forward flows on A-phase and B-phase feeding the ABG fault on L34 and the magnitudes of these forward IA and IB currents were more dominating than the reverse IC current.
- The mho impedance calculations fared better, as they remained secured for these double-circuit faults. T7P correctly detected the ABG fault on Line L34 by its forward-looking Zone 3 and detected the CG fault on Line L12 as reverse and outside the mho circles (Fig. 17) and, hence, remained secured. In addition, T1, T2, T3, and T4 calculated their respective mho impedance within their Zone 1 mho circles.
- The mho element FIDS logic at all terminals except Terminal T3 correctly asserted the FSC bit (indicating either a CG or ABG fault). FSC did not assert at T3 because FIDS logic did not enable. This was because the zero-sequence voltage and current magnitudes at T3 were not sufficient to reliably indicate that ground was involved in the fault.
- The directional element at T2 declared the actual forward fault on Line L12 as reverse. This was because the V2 and I2 relationship seen at Terminal T2 resembled that of a reverse SLG fault.
- From the previous observations, a common theme arises: sequence quantities seen at various terminals were unexpected. Consequently, relay elements that utilized sequence quantities operated unexpectedly.
- Drawing a system-wide view and analyzing on a per-phase basis (Fig. 12) helped understand the unconventional current flows captured in relay event reports for the double-circuit fault.
- Taking a system-wide view in the event viewer software by combining event reports from all of the terminals (Fig. 13) corroborated the current flow distribution presented in Fig. 12. This approach and the custom calculations were key in determining the fault type and whether ground was involved in the double-circuit fault.
- Meaningful information can only be extracted by combining multiple event reports if the event reports are time-synchronized. In turn, the event reports are time-synchronized only if the relays were time-synchronized with a high-accuracy time source (e.g., IRIG-B signal via a GPS clock) at the time of the fault. In this case study, we found that a couple of event reports were not time-synchronized. There are still ways to time-align the event reports manually. For instance, T4P was time-synchronized to T3P by adjusting the IC phasors so that they are 180 degrees out of phase with each other (as C-phase of Line L34 was unfaulted).
- T6P operation was triggered by T7P operation due to the use of a PUTT scheme. Both POTT and DCB schemes would have prevented T6P operation for this double-circuit fault.

- The 87L scheme for both Lines L567 and L34 disabled right after the double-circuit faults started. We took advantage of the already combined and time-aligned event reports to lay out the 87L communications channel health indicator bits (ROKX and ROKY) for all the relays. Systematically examining the ROK bits suggested issues with the communications equipment at the N45 substation housing the T4 and T5 relays. It was later found that these 87L schemes indeed used leased copper telecom lines at the N45 substation, which would be affected during nearby system ground faults. There is a project underway to upgrade 87L communication technology for these 69 kV lines.
- Even though 87L protection for Line L567 dropped out as the fault started, the line would have remained secured had 87L remained enabled. This is because the double-circuit fault is external to Line L567, and the KCL principle (current coming in is equal to current going out) will hold true in such a condition, as is evident from the current flows and phasors in Fig. 12 and Fig. 13, respectively.

X. Acknowledgment

The authors would like to thank Demetrios Tziouvaras for his guidance and support in writing this paper.

XI. References

[1] A. Guzmán, J. Roberts, and D. Hou, "New Ground Directional Elements Operate Reliably for Changing System Conditions," proceedings of the 51st Annual Georgia Tech Protective Relaying Conference, Atlanta, GA, April 1997.

[2] J. Roberts and A. Guzmán, "Directional Element Design and Evaluation," proceedings of the 21st Annual Western Protective Relay Conference, Spokane, WA, October 1994.

[3] K. Zimmerman and D. Costello, "Fundamentals and Improvements for Directional Relays," proceedings of the 64th Annual Conference for Protective Relay Engineers, College Station, TX, April 2011.

[4] G. Alexander, "Revised Setting Guidelines for E32 in SEL Relays," AG2016-14. Available: https://selinc.com/.

[5] E. O. Schweitzer, III and J. Roberts, "Distance Relay Element Design," proceedings of the 46th Annual Conference for Protective Relay Engineers, College Station, TX, April 1993.

[6] D. Fentie, "Understanding the Dynamic Mho Distance Characteristic," proceedings of the 69th Annual Conference for Protective Relay Engineers, College Station, TX, April 2016.

[7] D. Costello and K. Zimmerman, "Determining the Faulted Phase," proceedings of the 36th Annual Western Protective Relay Conference, Spokane, WA, October 2009.

XII. Biographies

Ahsan Mirza is a team lead in the Transmission and Distribution Relays section of System Protection and Control Engineering at San Diego Gas & Electric. He leads a team of engineers and analysts responsible for creating and updating all relay settings for capital and maintenance projects, from 500 kV down to distribution reclosers at 12 kV or 4 kV. Ahsan previously worked in the System Protection Maintenance group on commissioning substation equipment and relay systems. He received his B.S. degree in Electrical Engineering from University of Illinois at Urbana-Champaign and is a registered Professional Engineer in the State of California.

Christopher Bolton joined San Diego Gas & Electric (SDG&E) in 2011 as an associate engineer, settling in Substation Engineering as his first permanent assignment. There, he worked on the Capital Projects team managing and providing engineering support for various greenfield and brownfield substation and synchronous condenser installations. In 2016, Chris transferred to the Substation Technical Analysis and Support team at Kearny Maintenance and Operations, where he managed the construction and commissioning of various greenfield and brownfield substation and synchronous condenser installations. He then took a position as team lead in System Protection Maintenance, where he supervised relay technicians responsible for installing, commissioning, and maintaining SDG&E's substation control and protection infrastructure. Most recently, Chris has assumed the position of manager of System Protection and Control Engineering, where he oversees the engineering of all SDG&E control and protection/automation equipment for electric infrastructure. Chris graduated with a B.S. degree in Electrical Engineering from California State Polytechnic University, Pomona, and is a licensed Professional Engineer in the State of California.

Girolamo Rosselli received his B.S. degree in Electrical Engineering from the University of Illinois in 1978. Upon graduation, he was hired by Commonwealth Edison Company, where he worked on the planning side of the 12 kV overhead and underground distribution systems, as well as on electrical planning for high-rise buildings in central Chicago. He joined San Diego Gas & Electric as a substation engineer in 1981. In 1985, he joined the System Protection group, where he stayed until his retirement in August 2017. One of his major accomplishments is the coordination of the transmission and sub-transmission systems of the island of Guam. He published an article on 500 kV series capacitors in T&D World Magazine in 1987. He is a former member of the Western Protective Relay Conference (WPRC) program committee and has presented several papers at WPRC and Georgia Tech relay conferences. He received the Walter Elmore Best Paper Award in 2005 from the Georgia Institute of Technology. He is a life member and former chairman of IEEE/PES Society San Diego Chapter, and a Registered Professional Engineer in the State of California. He received three U.S. patents in 2016 and 2017 (US 9444245B2, US 9529028B2, and US 9612268B2). He started a consultant business, Rosselli Utilities Services LLC (RUS Engineering), in 2015.

Sergio Flores received his B.S. degree in Electrical Engineering from the University of Nevada, Las Vegas, in 2012 and a certificate in Power Systems from the University of California, San Diego, in 2016. He joined San Diego Gas & Electric in 2013 as an associate engineer with rotations in Smart Grid, District Engineering, and System Protection. Since 2014, he has been in the System Protection group, where he is a senior engineer. He is a Registered Professional Engineer in the State of California.

Amanvir Sudan received his bachelor of engineering degree in electrical and electronics engineering in 2011 from Panjab University in India. He then received his masters of science degree in electrical engineering, with a power system emphasis, in 2013 from Washington State University in the United States. Amanvir joined Schweitzer Engineering Laboratories, Inc. (SEL) in 2012 as an electrical engineering intern for the engineering services division, where his focus was automation. Since January 2014, Amanvir has been working as an application engineer in protection in the sales and customer service division of SEL and supports SEL customers in the southwest region of the United States.